MICHIGAN STATE
UNIVERSITY

National Superconducting Cyclotron Laboratory

SINGLE-NEUTRON KNOCKOUT FROM ^{34,35}Si AND ^{37}S

J. ENDERS, A. BAUER, D. BAZIN, A. BONACCORSO, B.A. BROWN, T. GLASMACHER, P.G. HANSEN, V. MADDALENA, K.L. MILLER, A. NAVIN, B.M. SHERRILL, J.A. TOSTEVIN

NSCL

MSUCL-1223 DECEMBER 2001

Single-neutron knockout from ^{34,35}Si and ^{37}S

J. Enders,[1] A. Bauer,[1,2,*] D. Bazin,[1] A. Bonaccorso,[3] B. A. Brown,[1,2] T. Glasmacher,[1,2] P. G. Hansen,[1,2] V. Maddalena,[1,2] K. L. Miller,[1,2] A. Navin,[1,†] B. M. Sherrill,[1,2] J. A. Tostevin,[4]

[1]*National Superconducting Cyclotron Laboratory, Michigan State University, East Lansing, Michigan 48824-1321*

[2]*Department of Physics and Astronomy, Michigan State University, East Lansing, Michigan 48824-1116*

[3]*Istituto Nazionale di Fisica Nucleare, Sezione di Pisa, 56100 Pisa, Italy*

[4]*Department of Physics, School of Physics and Chemistry, University of Surrey, Guildford, Surrey, GU2 7XH, United Kingdom*

(December 14, 2001)

Abstract

Results of single-neutron knockout experiments from ^{34,35}Si at 73 A MeV and from ^{37}S at 69 A MeV on a Be target are reported. The final states in the reaction residues have been identified by measuring γ rays in coincidence with the $(A-1)$ fragments. The results are compared with predictions based on the many-body shell model combined with eikonal and transfer-to-the-continuum reaction models. For the ^{9}Be(^{34}Si,^{33}Si+γ)X reaction, the measured parallel-momentum distributions of the reaction residues demon-

*Research experience for undergraduates (REU) student from Amherst College, Amherst, MA; present address: Yale University, New Haven, CT.

†Permanent address: Nuclear Physics Division, Bhabha Atomic Research Centre, Trombay, Mumbai, India.

strate the orbital-angular-momentum assignments $\ell = 2$, 0, 2 to levels at 0, 1.010 and 4.32 MeV (adopted values). The measured absolute spectroscopic factors exhaust a large fraction of the sum rules for a full ($N = 20$) *sd* shell. We also give results for the absolute and relative positions of the parallel-momentum distributions and present experimental and theoretical results for the complex spectra of the ^{9}Be(^{35}Si,^{34}Si+γ)X reaction. The measured inclusive cross section of 106(19) mb agrees well with the theoretical value of 98 mb, but more detailed conclusions are not possible. For the inclusive reaction ^{9}Be(^{37}S,^{36}S)X a cross section of 99(12) mb is found compared to the theoretical prediction of 85 mb where only final states with spectroscopic factors greater than 0.03 have been included.

I. INTRODUCTION

The very neutron rich nuclei show a number of examples where weakening of the shell gaps and correlations bring intruder states close to or below what would be the ground state in the usual model space, see Ref. [1]. A particularly interesting example occurs for the $N = 20$ isotones where ^{32}Mg and some of the neighboring nuclei are known to be strongly deformed. On the other hand, the nucleus with just two protons more, ^{34}Si, appears to be spherical as is borne out by the high energy, 3.328 MeV, of the 2^+ state [2]. The measured $B(E2)$ value from a Coulomb excitation experiment by Ibbotson *et al.* [3] could be interpreted in terms of a relatively large intruder contribution to the 2^+ state with the ground state being a pure $\nu(sd)^{12}$ $(0\hbar\omega)$ configuration corresponding to an $N = 20$ closed shell. The structure of the nucleus with one neutron less, ^{33}Si, was studied by Fifield *et al.* [4], who measured the ^{3}He pickup from a ^{36}S target and found strong cross sections to only three levels, the ground state, 1.06(2) and 4.32(3) MeV, respectively. The relative cross sections agreed with the interpretation of these as the $d_{3/2}$, $s_{1/2}$, and $d_{5/2}$ holes, respectively. Further support was found in a Coulomb excitation experiment by Pritychenko *et al.* [5] who observed population of a state given as 1.01 MeV in an intensity consistent with the $1s_{1/2}$ assignment from the shell model. A 4.3 MeV γ ray was assumed to arise from the excitation of two states with spins $3/2^+$ and $5/2^+$, although other reactions also could contribute at this energy. In the present work we have used the single-neutron knockout reaction ^{9}Be(^{34}Si,^{33}Si+γ)X to identify the main single-particle components of the knocked-out neutron by their measured ℓ values and absolute spectroscopic factors. Data were also taken for the corresponding reactions of ^{35}Si and ^{37}S.

The knockout reaction in inverse kinematics with radioactive beams at energies $E_{\rm kin} \geq 50\,A$ MeV is a technique that has been used [6–12] to identify single-particle configurations of rare isotopes. It seems that this technique can obtain results comparable to those traditionally associated with single-nucleon pickup reactions [13], however, the sensitivity is greatly increased, and one experiment has already been carried out with an incident beam

of less than one atom/s [11]. At the higher energies involved, semi-classical theories (e.g. based on the eikonal approximation) can be used which are simpler and have fewer free parameters. Nevertheless, these theories have the potential for yielding precise spectroscopic factors which provide quantitative information on the composition of the wave functions of the initial and final states involved.

In the knockout experiments, projectile residues from single-nucleon removal reactions are detected in a high-resolution spectrometer that identifies the outgoing fragment and measures its momentum distribution with high resolution. (The parallel-momentum spectrum plays the same role for the angular momentum identification as the angular distribution in transfer reactions.) A coincidence between the fragments at the focal plane of the spectrograph and the γ rays detected close to the target identifies individual excited states. Similar single-neutron knockout reactions have been used – without the detection of γ rays – to establish the occurrence of halos characterized by narrow momentum spectra reflecting the large spatial extent of the wave halo function [14]. (An application for proton halos with detection of the γ rays is demonstrated in [6].) The method is simplest to apply in the case of nuclei close to the limit of stability (the "drip line") where only a few bound final states are possible. The intensity balance for a case with many final states can be very difficult, at least until high-resolution γ detectors become available for this kind of experiment.

An additional motivation behind the present work was to extend our understanding of this spectroscopic tool. The data given below are the first obtained for nuclear masses $A > 30$ and for well-bound systems with a high density of final states. Previous experiments had explored the p and sd proton and neutron shells and had given examples of momentum distributions for the $0p_{3/2}$, $0p_{1/2}$, $1s_{1/2}$, and $0d_{5/2}$ orbitals. Although these in general agreed well with calculations within an eikonal approach [15,16], better data showed a low-momentum tail in the s-wave knockout that can only be accounted for in calculations that go beyond eikonal theory [17,18]. Other possible modifications to calculated momentum distributions are suggested within the transfer to the continuum (TC) model of Ref. [19]. This model predicts different neutron momentum distributions for states with the same ℓ

and different j [20]. Such a behavior has not been observed up to now, but data for the $0d_{3/2}$, $0d_{5/2}$ pair could test this.

The organization of this paper is as follows: After summarizing the experimental procedure in Sec. II, the fundamentals of the reaction and structure models will be reviewed in Sec. III. Section IV contains the presentation and discussion of the results for the neutron knockout from ^{34}Si, and the results for the knockout from ^{35}Si and ^{37}S are found in Sec. V.

II. EXPERIMENTAL TECHNIQUE

The experimental setup has been described previously in Ref. [11]. The unstable ^{34,35}Si and ^{37}S beams were produced by fragmentation of a 40 pnA beam of ^{40}Ar at 100 A MeV, which was produced by the K1200 cyclotron of the National Superconducting Cyclotron Laboratory (NSCL) at Michigan State University. The rare-isotope beams were purified in the A1200 fragment separator and guided to the secondary target area at the high-resolution S800 spectrograph [21] operated in energy-loss mode. The secondary target (^{9}Be, 93 mg/cm^2) was surrounded by an array of NaI(Tl) scintillators [22] to detect γ rays emitted by the reaction residues. The reaction residues were identified by momentum, energy loss, and time of flight in the detector system at the focal plane of the S800 spectrograph [23]. The energy loss in the target was approximately 4 A MeV.

Table I summarizes the main characteristics of the secondary beams used in the experiment. The cross sections for neutron removal have been calculated from the number of residues identified in the focal plane of the S800 spectrograph taking the geometrical acceptance of the spectrograph into account ($\pm 5^\circ$ horizontal, $\pm 3.5^\circ$ vertical at the central momentum). The main error sources in the determination of the cross sections stem from the software cuts in the particle identification (10%), the stability of the rate of incident particles from the beam purity (3% for ^{34}Si, 5% for ^{35}Si), and from a general uncertainty of the thickness and homogeneity of the secondary target (5%). In addition to that, not all residues could be detected due to the finite momentum acceptance ($\Delta p/p = \pm 2.5\%$) of

the spectrograph, therefore there is an uncertainty associated with the estimation of the undetected fragments. It is assumed that the systematic errors are independent, and they have been added in quadrature.

III. THEORETICAL ANALYSIS

The cross section $\sigma(J_n^\pi)$ for removing a single particle with quantum numbers $(N\ell j)$ and for leaving the core in a specific final state (J_n^π) can be decomposed [7] into a structure part and a reaction part

$$\sigma(J^\pi) = \sum_j C^2S(j, J^\pi) \cdot \sigma_{\rm sp}(j, B)\,. \tag{1}$$

Here, B denotes the effective binding energy of the removed neutron given by $B = S_{\rm n} + E_{\rm x}(J^\pi)$ with the neutron separation energy $S_{\rm n}$ and the excitation energy of the final state of the core $E_{\rm x}(J^\pi)$. (The neutron separation energies of the isotopes studied here are $S_{\rm n}(^{35}{\rm Si})$ = 2.75 MeV, $S_{\rm n}(^{34}{\rm Si})$ = 7.36 MeV, and $S_{\rm n}(^{37}{\rm S})$ = 4.30 MeV.) The structure information is contained in the spectroscopic factors C^2S, and $\sigma_{\rm sp}(j, B)$ is the theoretical single-particle reaction cross section assuming a spectroscopic factor of unity.

A. Nuclear structure and spectroscopic factors

For the positive parity states in ^{33}Si and ^{34}Si we use the *sd* model space with the USD effective interaction [24]. The valence configurations are of $\pi(sd)^6\,\nu(sd)^{11}$ and $\pi(sd)^6\,\nu(sd)^{12}$, respectively. Energy levels for all *sd*-shell nuclei obtained with USD are given in [25]. The ^{35}Si ground state is obtained in the $sd-pf$ model space with configurations $\pi(sd)^6\,\nu(sd)^{12}\,\nu(pf)^1$, and the ^{34}Si negative-parity excited states have the configurations $\pi(sd)^6\,\nu(sd)^{11}\,\nu(pf)^1$. These configurations for the positive and negative parity states in ^{34}Si provide the complete set of low-lying states that can be reached by one-neutron knock-out from ^{35}Si. The $sd-pf$ Hamiltonian is WBMB which was developed to study the island of inversion around ^{32}Mg [26], and has more recently been applied to more neutron-rich

nuclei [27]. The WBMB Hamiltonian consists of the USD interaction for the *sd*-shell part of the Hamiltonian and a potential model for the $sd-pf$ cross-shell matrix elements. The single-particle energies and the parameters of the potential were obtained from the properties of nuclei near ^{40}Ca. All shell-model calculations were carried out with the program Oxbash [28].

B. Reaction cross sections

1. The eikonal model

The single-particle reaction cross sections have been calculated within the eikonal approach of Ref. [17] using the same parameters as in previous studies. We note that since only the reaction residue (in coincidence with γ rays) is detected, the measured knockout cross section consists of the incoherent sum of contributions from stripping (absorption of the removed neutron in the target) and diffraction dissociation (elastic break-up). These contributions are determined independently from the core-target and neutron-target S-matrices, which are calculated within Glauber theory. The wave function of the composite (core-neutron) state was obtained from a Woods-Saxon potential with radius and diffuseness parameters chosen to be $r_0 = 1.25$ fm and $a = 0.7$ fm as in the preceding studies. We point out that for the rather well-bound nuclei discussed here, the stripping contribution is approximately 75% of the cross section. For details, see [11,17] and references therein.

The parallel-momentum distributions of the residues were calculated in the black-disk description [15] with the effective interaction radii chosen to reproduce the reaction cross sections of the free constituents. This is permissible because the momentum spectra are relatively insensitive to the details of the interaction in the direction perpendicular to the beam direction, but very sensitive to the orbital angular momentum ℓ of the knocked-out particle and its binding energy B. Thus the comparison of the measured momentum distributions with the shapes from theory can provide ℓ-value assignments. Since, at a more

detailed level, using the sudden approximation for the interaction of the projectile in the eikonal model does not conserve energy, details of the momentum distributions will deviate slightly from these theoretical expectations [18].

2. Transfer to the continuum model

The transfer to the continuum (TC) model [19] offers an alternative method to calculate momentum distributions and total cross sections for nucleon removal. A generalization of the semi-classical formalism for transfer reactions between bound states, it includes a more complete dynamical treatment of the neutron motion than in the eikonal model. Spin coupling between initial and final states is also more readily included. These effects are expressed in terms of the optical model S-matrix between the removed neutron and the target, evaluated at the energy of the breakup neutron in the final continuum state with respect to the target. The relevant formulae are presented in Ref. [20] where the dependence of the spin coupling coefficients on the angular momentum, spin and neutron final energy were shown to introduce distortions in the calculated neutron parallel momentum distributions. Here these neutron distributions are translated into core momentum distributions using momentum conservation, but with the assumption that the kinematics are those of elastic breakup and that target recoil energies can be neglected for the relevant peripheral core-target trajectories.

IV. THE ^{9}Be(^{34}Si,^{33}Si)X REACTION

A. Analysis of the γ–ray spectrum

After the identification of the reaction residues in the spectrograph, the γ-ray spectrum in coincidence with the detected ^{33}Si particles could be constructed. It identifies the different final states populated in the process. The distribution in Fig. 1 shows the spectrum as a function of the reconstructed center-of-mass energy normalized to the number of de-

tected breakup fragments. One recognizes two peaks in the spectrum, of which the lowest clearly corresponds to the 1.010 MeV state [4] of which the γ ray is known from previous experiments [5,29,30] while the second is a peak near 4.3 MeV. Because the photomultiplier tubes (PMTs) of the NaI(Tl) detector system are very sensitive to the magnetic field of the S800 spectrograph and have been calibrated for a slightly different magnetic field setting of the spectrograph, we have used the the precisely known 1.010 MeV γ ray to recalibrate the spectrum. The second peak is then at 4.29(14) MeV, where the (conservative) error corresponds to the full change of 3.3% in PMT gain between the settings for knockout from ^{34}Si and ^{35}Si. This is in good agreement with the energy of the state observed by Fifield *et al.* [4] at 4.32(3) MeV, and we have used this, more accurate, result as the adopted value in the present work. We interpret this γ ray as representing a single transition from the $5/2^+$ level, but contributions from other unresolved transitions cannot be excluded. (A $3/2^+$ state should be present nearby [5], but is expected theoretically to have a low cross section.)

In order to quantify the population of these states, simulations with the code GEANT 3 [31] have been carried out. These take into account the Doppler shift arising from the projectile velocity ($\beta \approx 0.36$) and generate the energy deposited in the detectors. The simulations also include the finite position resolution of the position-sensitive NaI(Tl) detector array. The analysis of these pseudo data gave rise to line shapes that were fitted to match the experimental spectrum as shown by the dashed curves in Fig. 1. (These shapes clearly must differ from what would be measured with a calibration source at rest.) As in our previous experiments, the experimental γ spectra contained a continuous distribution of clearly beam-related events, which for our purposes represent an unavoidable background [9,32]. This was parameterized as a single exponential function, see the dotted line in Fig. 1. Its shape and absolute intensity agrees within about 20% with that observed more directly in the single-neutron removal from ^{12}Be and ^{16}C, where the residues have no high-energy γ rays. The overall fit of the simulated line shapes and the continuous background is indicated by the double line in Fig. 1; it agrees nicely with the measured data.

There is no evidence for other γ transitions. Since the highest level at 4.32 MeV is just

below the neutron threshold of ^{33}Si at $S_n = 4.483(16)$ MeV, indirect feeding from unobserved higher levels can be excluded. The absolute experimental branching ratios of 34(2)% for the 1.010 MeV level and 12(2)% for the 4.32 MeV level should therefore be very reliable. They have been used to derive the partial cross sections discussed in the following subsection.

B. Partial reaction cross sections

In order to obtain the partial reaction cross sections from the measured branching ratios one has to include spectrograph angular and momentum acceptance corrections. For the ^{9}Be(^{34}Si,^{33}Si)X reaction angular acceptance corrections have been obtained from Monte-Carlo simulations using the measured (raw) parallel and transverse momentum distributions; they could be quantified to be less than 3%. An additional systematic error of 5% was added to take the limited momentum acceptance into account. This rough estimate for the momentum acceptance has been made since there is no reliable way to extrapolate the measured momentum distributions as will be discussed later.

The comparison of theoretical predictions and experimental results is shown in Table II, which contains information about the excitation energy of the final state E_x, the total angular momentum and parity of the populated state J^π, the quantum numbers $(N\ell j)$ of the removed neutron as predicted from the shell model, the single-particle removal cross sections for stripping σ_{sp}^{str} and diffraction σ_{sp}^{diff} as calculated within the eikonal model ('Eik', cf. Refs. [12,17]) and the transfer-to-the-continuum model ('TC', see [19,20]). The spectroscopic factor C^2S, the total theoretical neutron-knockout cross section σ_{Th} for the two reaction models, and the reaction cross section measured experimentally σ_{Exp} complete the table.

In agreement with [4] we interpret the three levels observed in ^{33}Si as the $J^\pi = 3/2^+$, $1/2^+$, and $5/2^+$ states, respectively. These assignments find further support in the measured values $\ell = 2$, 0, 2, respectively, deduced from the longitudinal momentum distributions discussed below. The assignment of $J^\pi = 3/2^+$ to the ground state also seems likely from the states in ^{33}P populated in β decay [33]. As can be seen from Table II, the

agreement between theoretical prediction $\sigma_{\rm Th}$ (for both reaction models) and experimental observation $\sigma_{\rm Exp}$ is very good. The total cross sections obtained from theory (113 mb when using the eikonal model, 96 mb for the transfer to continuum model) compare well with the measured inclusive cross section of 123(14) mb.

An experimentally known $(7/2^-)$ state [29,34] at 1435 keV in ^{33}Si is an intruder from the pf-shell and not contained in the model space. There is also no experimental evidence for the predicted $7/2^+$ state which should arise from a $(2^+ \otimes 3/2^+)$ configuration.

C. Spectroscopic factors

From the measured exclusive reaction cross sections one can extract experimental values for the spectroscopic factors. For consistency with previous analyses, we have used the single-particle estimates from the eikonal approach of Ref. [17] only. Table III compares the predictions of the shell model with the experimental spectroscopic factors.

It is interesting to point out that the shell closure at $N = 20$ is still very well preserved for the ground state of ^{34}Si – in agreement with theory [2,3,26,35,36]. This can be seen from the high spectroscopic factor for the branch to the ground state of ^{33}Si: The sum rule $\sum C^2S \leq (2j+1)$ is, within the experimental error, exhausted by the branch to the ground state. Moreover, an $s_{1/2}$ removal leads also with maximum strength to the first excited state at 1010 keV. The somewhat lower value for the reaction to the $0d_{5/2}$ state seems to be in line with what is seen for deep hole states in other cases [12]. The data set presented here contains the largest values of spectroscopic factors analyzed in knockout reactions from fast unstable beams so far. The data allow us to test structure vs. reaction in an extended regime of spectroscopic factors. Figure 2 shows a plot of spectroscopic factors from knockout experiments in comparison with predictions from many-particle shell-model calculations based of effective interactions, including the new data from ^{34}Si neutron removal (full symbols). A dashed line with slope of unity is drawn to guide the eye. It is seen to represent the results rather well. The fact that there is good agreement between the

extracted spectroscopic factors and the theoretical ones, which are expected to be reliable in these shells, is evidence that the knockout technique does provide spectroscopic information.

D. Momentum distributions

1. Experimental results

The momentum distributions of residues left in a specific final state after the knockout process can be obtained from the coincident γ-ray spectrum by applying software cuts in the γ-ray energies. These were placed at different energy regions so that underlying background effects and contributions from γ rays with higher energies could be subtracted to give the clean contribution coincident with a given transition. Similarly, the distribution for the ground state is deduced by subtracting on an absolute scale the momentum distributions associated with the excited final states from the inclusive momentum distribution. Angular acceptance corrections were applied as described above; they are important at the edges of the momentum distributions only. In the present case, the total angular acceptance correction amounted to less than 3%, which is small compared to other systematic errors of the method.

Figure 3 shows the extracted momentum distribution as full data points for the branch to the ground state of ^{33}Si with proposed $J^\pi = 3/2^+$ on the left panel. The middle and right part of Fig. 3 show the distributions associated with the excited states at 1.010 MeV and 4.32(3) MeV, respectively. In all three cases, the major part of the momentum spectrum is well within the momentum acceptance window of the spectrograph but with a clear tail toward lower momenta. The different widths suggest the angular momentum assignments $\ell = 2$, 0, 2, respectively. This is borne out by the theoretical calculations of the momentum distributions discussed in the following.

2. Comparison with the eikonal approach

Figure 3 compares the experimental momentum distributions with calculations for the removal of a $1s$ or a $0d$ neutron. These are based on the black-disk eikonal model of Ref. [15], and as in the previous work [6,8–11] the distribution was based on an integration over the reaction zone. (The analytical expressions given in [15] approximate the wave function by its value at the center of the target.) The effective radii were adjusted to reproduce the reaction cross sections of the neutron, respectively the residue, with the target. This procedure gives accurate longitudinal momentum distributions because the precise shape of the interaction at the surface is important only for the transverse momentum components. (In fact, even the absolute values of the cross sections obtained in this way agree rather well with those calculated with more accurate profile functions.)

We now turn to the information provided by the shapes of the distributions (mainly the ℓ values) and by their location relative to each other and to the momentum of the incident beam. The calculated momentum spectra for assumed values of ℓ of 0 and 2 were scaled to match the data in relative height and, with the appropriate Lorentz transformation, in position. The shapes clearly provide the assignments of $\ell = 2$, 0, 2 to the ground state, 1.01 and 4.32 MeV excited states, respectively and underpin the assignments given above. The ground state is the first case of a $d_{3/2}$ neutron orbital observed with the knockout technique. The narrow width found for the state at 1.01 MeV (middle panel of Fig. 3) clearly identifies it as an ℓ=0 excitation, in agreement with expectations from the shell model. In this case, there is evidence for a low-momentum tail similar to the one reported for the halo of ^{15}C by Tostevin *et al.* [18], who interpreted it as arising from energy conservation in the diffractive breakup channel.

The knowledge of the absolute momenta involved in the reaction is limited by hysteresis effects which lead to an uncertainty of approximately 0.1% on the effective magnetic field. From a measurement with a field setting that allowed the incident beam (with the Be target in place) to be detected in the spectrograph, it is calculated that if the average momentum

exchange is assumed to be zero, as required by the sudden approximation, the residues should emerge centered at 12.27(3) GeV/c. This agrees well with the observed values for the three states, given in Fig. 3, of 12.200(4), 12.250(3), and 12.250(10) GeV/c, where the errors are statistical only. This result is consistent with the analysis (based on an eikonal model and the sudden approximation) underlying our previous experiments [6–12]. We note in passing that the question of the relative shifts in velocity of the reaction residues in Coulomb and nuclear breakup reactions has been discussed in [37,38], where the latter found no evidence for the so-called "postacceleration effect".

The fact that the distributions in Fig. 3 were taken at one setting of the spectrograph and represent subsets sorted on the basis of coincidences with γ rays permits a more accurate statement about *relative* momenta. The distribution associated with the $3/2^+$ ground state has a lower parallel momentum than those associated with the two higher levels. The shift of $-50(5)$ MeV/c relative to the $1/2^+$ state is most accurately determined. A similar effect was seen in the recent experiment on ^{15}C, except that in this case [18] it was the excited level at 6.09 MeV that had a downshift of 8 MeV/c relative to the ground state at a total ^{14}C momentum of 4.51 GeV/c. The origin of these (small) shifts remains an interesting puzzle. The fact that opposite signs were obtained in the two cases seems to rule out a simple connection to energy and momentum conservation laws.

3. Transfer-to-the-continuum model and optical potential

Figure 4 compares the measured parallel-momentum distributions (full points) and the transfer to the continuum (TC) calculations. These have been performed at an incident energy of 70.6 A MeV, such that the centroid of the calculated $s_{1/2}$ distribution coincides with that of the data. The $d_{3/2}$ and $d_{5/2}$ distributions were obtained without further adjustment. The centroids of both distributions are in good agreement with the data, and the position of the peak of the $d_{3/2}$ distribution, which is shifted with respect to the other two distributions, originates from the asymmetry induced by the spin coupling term [20]. While the maximum

of the calculated s-wave removal distribution agrees with the experimental data without further adjustment, the $d_{3/2}$ and $d_{5/2}$ distributions have been rescaled by 1.32 and 0.7, respectively. The neutron optical potential used was close to those of Ref. [20] for a neutron-target energy of about 70 MeV. An imaginary volume term has been added whose effect is to improve agreement between the calculated and experimental free neutron-target cross sections. The use of a spin-orbit interaction is essential in producing the difference between the $d_{3/2}$ and $d_{5/2}$ distributions. The core survival probability, at each impact parameter, was parameterized with a smooth cut-off function as in [20] with a strong absorption radius $R_s = 7.35$ fm and diffuseness of $a = 0.6$ fm. The absolute cross section values and optical potential parameters are given in Table II and Table IV, respectively.

The total cross sections, obtained by integration of the momentum distributions, are in good agreement with the eikonal values, see Table II. The breakup cross sections from the s-state are the same, which shows a certain insensitivity to the details of the neutron-target S-matrix. For knockout from d-orbitals the values from the TC model are somewhat smaller values than those from the eikonal model [40].

V. THE ^{9}Be(^{35}Si,^{34}Si)X AND THE ^{9}Be(^{37}S,^{36}S)X REACTIONS

Figure 5 shows the measured γ-ray spectrum for the ^{9}Be(^{35}Si,^{34}Si+γ)X reaction. The histogram displays the measured data. One recognizes four structures around 500 keV, 900 keV, 3300 keV and 4200 keV. A careful inspection of the spectrum, however, reveals that the data cannot be described appropriately by these four transitions only plus a single exponential function to model the background. One would have to assume a slope and an absolute amount of the continuous background distribution that would deviate significantly from previous measurements [11,32] and also from the results obtained for ^{34}Si.

In addition to the aforementioned four transitions, further transitions in ^{34}Si are known from the $\beta\gamma$ study of Ref. [30]. However, an unambiguous placement of the γ-rays of [30] is not always possible, neither is there a one-to-one correspondence between the proposed

excited states and the shell-model calculation. Using the spectroscopic information of [30], the γ-ray spectrum in coincidence with the reaction residues has been fitted using a single exponential function for the description of the background and eight simulated line shapes. The results are shown in Fig. 5 as dotted and dashed lines, respectively. In this case, the parameterization of the continuous exponential distribution yields values comparable to those deduced for the neutron removal from ^{34}Si. However, a disagreement between the overall fit (double solid line in Fig. 5) and the measured data is clearly visible and indicates the possibility of an even more complex spectrum.

Table V shows the quantitative results of the fit shown in Fig. 5. The γ-ray energy E_γ is given with the possible quantum numbers and excitation energies of the initial and final states ($J^\pi_{i/f}; E_{x,i/f}$) and the ratio b, which describes how often a γ ray of this energy is observed in coincidence with a reaction residue. If all initial and final states are known, it is possible to deduce from this the exclusive reaction cross sections (not including acceptance corrections) by subtraction, but due to uncertainties in the level scheme (question marks in Table V) this is not yet possible. Although the transitions relating the 0^+_1, 2^+_1, and 3^-_1 states stand out in the measured γ-ray spectrum, it is not possible to extract partial cross sections due to side feeding of these states.

Table VI lists (in analogy to Table II) the predictions for single-particle cross sections as calculated within the eikonal model and the spectroscopic factors from the shell model. As can be seen, about 80% of the total cross section can be attributed to the removal of a neutron in a d or an s orbital whereas only 20% are expected to result from f-wave knockout. The theoretical inclusive cross section of 98 mb from summing over all states with non-negligible spectoscopic factors below the neutron separation energy agrees well with the experimental value of 106(19) mb.

Figure 6 shows the measured inclusive momentum distributions both for the knockout from ^{34}Si (upper part) and ^{35}Si (lower part). One recognizes a striking similarity between these spectra which indicates that the dominant reaction channels contributing are similar in both cases. A closer inspection reveals that the inclusive distribution for the knockout from

^{34}Si is actually wider than the momentum spectrum of the ^{35}Si breakup, and a particularly wide component from the anticipated f-wave removal from ^{35}Si is not visible in the spectra. The different widths of the distributions cannot be attributed to the differences in the neutron separation energies [$S_n(^{35}\mathrm{Si}) = 2.75$ MeV, $S_n(^{34}\mathrm{Si}) = 7.36$ MeV] since the effective binding energies $B = S_n + E_x$ are comparable for similar orbitals.

Similarly, data have been taken for the neutron knockout from ^{37}S. The residual nucleus ^{36}S has the very high neutron separation energy of 9.89 MeV. From a shell model calculation, 23 states are expected to be populated by the knockout process with spectroscopic factors greater than 0.03. In a calculation similar to that of Table VI, the partial cross sections can be obtained for each of these final states, leading to a total (inclusive) cross section of 85 mb. This value compares well with the experimental result of 99(12) mb. The γ-ray data in coincidence with the residues could not be evaluated quantitatively due to pile-up effects induced by the high incident beam rate and the high complexity of the spectrum.

VI. CONCLUSION AND OUTLOOK

A large-acceptance spectrograph and an array of efficient and position-sensitive NaI(Tl) γ-ray detectors have been used to study neutron-knockout reactions on ^{34}Si, ^{35}Si, and ^{37}S. The main results concern the ^{9}Be(^{34}Si,^{33}Si+γ)X reaction, in which three final states are populated, the ground state and levels at 1.010 and 4.32(3) MeV (adopted values). The parallel-momentum distributions of the reaction residues demonstrate the orbital-angular-momentum assignments $\ell = 2, 0, 2$. The absolute spectroscopic factors exhaust large fractions of the sum rules for a full ($N = 20$) sd shell and prove that the levels to a good approximation represent the single-particle holes $0d_{3/2}$, $1s_{1/2}$, and $0d_{5/2}$, respectively. The results show that the magic $N = 20$ shell gap is preserved for silicon ($Z = 14$) while it is known to break down for the nucleus with two protons less, magnesium ($Z = 12$).

An interesting result concerns the position of the parallel-momentum distributions. In the sudden approximation, the average velocity would be the same as that of the incident beam.

This was determined in a separate measurement and corresponds to a residue momentum of 12.27(3) GeV/c. In fact, the three measured distributions are within two standard deviations of this. It is, however, possible to make more precise statements concerning the *relative* momenta of the three distributions. We find that the $3/2^+$ ground state is formed with on the average 50(5) MeV/c less momentum than the $1/2^+$ level, and the shift relative to the $5/2^+$ level is about the same magnitude. A similar effect, smaller and of the opposite sign, was recently seen in reactions of ^{15}C [18]. The origin of this shift is unknown, but an explanation in terms of a simple kinematical effect seems excluded since the level in ^{33}Si with the lowest excitation energy is the one that appears with the lowest velocity.

The transfer-to-the-continuum model obtains shifts and asymmetries that are qualitatively in good agreement with the data. In contrast to the eikonal approach discussed above, the TC model uses the same beam energy to produce momentum spectra in agreement with the data for all three measured final states.

The much more complex γ-ray spectrum of the ^{9}Be(^{35}Si,^{34}Si+γ)X reaction seems to represent the limit of what can be done with NaI(Tl) detectors. An array of high-resolution segmented germanium detectors [41] designed to provide precise Doppler corrections is now being commissioned at the NSCL.

ACKNOWLEDGMENTS

We thank D. W. Anthony, T. Aumann, T. Baumann, Y. Blumenfeld, R. W. Ibbotson, P. A. Lofy, T. Nakamura, B. V. Pritychenko, E. J. Spears, M. Steiner, A. Wagner, and J. E. Yurkon for their assistance during the experiment. This work was supported by the U. S. National Science Foundation through grants PHY 95 28844 and PHY 00 70911, and by the UK EPSRC Grant GR/M 82141 (for J.A.T.).

REFERENCES

[1] B. A. Brown, Prog. Part. Nucl. Phys. **47**, 517 (2001).

[2] P. Baumann, A. Huck, G. Klotz, A. Knipper, G. Walter, G. Marguier, H. L. Ravn, C. Richard–Serre, A. Poves, and J. Retamosa, Phys. Lett. B **228**, 458 (1989).

[3] R. W. Ibbotson, T. Glasmacher, B. A. Brown, L. Chen, M. J. Chromik, P. D. Cottle, M. Fauerbach, K. W. Kemper, D. J. Morrissey, H. Scheit, and M. Thoennessen, Phys. Rev. Lett. **80**, 2081 (1998).

[4] L. K. Fifield, C. L. Woods, R. A. Bark, P. V. Drumm, and M. A. C. Hotchkis, Nucl. Phys. A **440**, 531 (1985).

[5] B. V. Pritychenko, T. Glasmacher, B. A. Brown, P. D. Cottle, R. W. Ibbotson, K. W. Kemper, and H. Scheit, Phys. Rev. C **62**, 051601(R) (2000).

[6] A. Navin, D. Bazin, B. A. Brown, B. Davids, G. Gervais, T. Glasmacher, K. Govaert, P. G. Hansen, M. Hellström, R. W. Ibbotson, V. Maddalena, B. Pritychenko, H. Scheit, B. M. Sherrill, M. Steiner, J. A. Tostevin, and J. Yurkon, Phys. Rev. Lett. **81**, 5089 (1998).

[7] J.A. Tostevin, J. Phys. G **25**, 735 (1999).

[8] T. Aumann, A. Navin, D. P. Balamuth, D. Bazin, B. Blank, B. A. Brown, J. E. Bush, J. A. Caggiano, B. Davids, T. Glasmacher, V. Guimarães, P. G. Hansen, R. W. Ibbotson, D. Karnes, J. J. Kolata, V. Maddalena, B. Pritychenko, H. Scheit, B. M. Sherrill, and J. A. Tostevin, Phys. Rev. Lett. **84**, 35 (2000).

[9] A. Navin, D. W. Anthony, T. Aumann, T. Baumann, D. Bazin, Y. Blumenfeld, B. A. Brown, T. Glasmacher, P. G. Hansen, R. W. Ibbotson, P. A. Lofy, V. Maddalena, K. Miller, T. Nakamura, B. V. Pritychenko, B. M. Sherrill, E. Spears, M. Steiner, J. A. Tostevin, J. Yurkon, and A. Wagner, Phys. Rev. Lett. **85**, 266 (2000).

[10] V. Guimarães, J. J. Kolata, D. Bazin, B. Blank, B. A. Brown, T. Glasmacher, P. G. Hansen, R. W. Ibbotson, D. Karnes, V. Maddalena, A. Navin, B. Pritychenko, B. M. Sherrill, D. P. Balamuth, and J. E. Bush, Phys. Rev. C **61**, 064609 (2000).

[11] V. Maddalena, T. Aumann, D. Bazin, B. A. Brown, J. A. Caggiano, B. Davids, T. Glasmacher, P. G. Hansen, R. W. Ibbotson, A. Navin, B. V. Pritychenko, H. Scheit, B. M. Sherrill, M. Steiner, J. A. Tostevin, and J. Yurkon, Phys. Rev. C **63**, 024613 (2001).

[12] P. G. Hansen and B. M. Sherrill, Nucl. Phys. A **693**, 133–168 (2001).

[13] G. R. Satchler, Direct Nuclear Reactions (University Press, Oxford, 1983).

[14] T. Kobayashi, O. Yamakawa, K. Omata, K. Sugimoto, T. Shimoda, N. Takahashi, and I. Tanihata, Phys. Rev. Lett. **60**, 2599 (1988).

[15] P. G. Hansen, Phys. Rev. Lett. **77**, 1016 (1996).

[16] H. Esbensen, Phys. Rev. C **53**, 2007 (1996).

[17] J. A. Tostevin, Nucl. Phys. A **682**, 320c (2001).

[18] J. A. Tostevin, D. Bazin, B. A. Brown, T. Glasmacher, P. G. Hansen, V. Maddalena, A. Navin, and B. M. Sherrill, in *Proceedings of the International Nuclear Physics Conference, Berkeley, 2001* (to be published)

[19] A. Bonaccorso and D. M. Brink, Phys. Rev. C **58**, 2864 (1998).

[20] A. Bonaccorso, Phys. Rev. C **60**, 054604 (1999).

[21] J. A. Caggiano, Ph.D. thesis, Michigan State University, 1999.

[22] H. Scheit, T. Glasmacher, R. W. Ibbotson, and P. G. Thirolf, Nucl. Instr. Methods in Phys. Res. A **422**, 124 (1999).

[23] J. Yurkon, D. Bazin, W. Benenson, D. J. Morrissey, B. M. Sherrill, D. Swan, and R.

Swanson, Nucl. Instr. Methods in Phys. Res. A **422**, 291 (1999).

[24] B. A. Brown and B. H. Wildenthal, Ann. Rev. Nucl. Part. Sci. 38, 29 (1988); B. H. Wildenthal, Prog. Part. Nucl. Phys. **11**, 5 (1984).

[25] http://www.nscl.edu/~brown/sde.htm

[26] E. K. Warburton, J. A. Becker, and B. A. Brown, Phys. Rev. C **41**, 1147 (1990).

[27] T. Siiskonen, P. O. Lipas, and J. Rikovska, Phys. Rev. C **60**, 034312 (1999).

[28] B. A. Brown, A. Etchegoyen, W. D. M. Rae, N. S. Godwin, W. A. Richter, C. H. Zimmerman, W. E. Ormand, and J. S. Winfield, MSU-NSCL Report No. 524, 1985.

[29] B. Fornal, R. H. Mayer, I. G. Bearden, P. Benet, R. Broda, P. J. Daly, Z. W. Grabowski, I. Ahmad, M. P. Carpenter, P. B. Fernandez, R. V. F. Janssens, T. L. Khoo, T. Lauritsen, E. F. Moore, and M. Drigert, Phys. Rev. C **49**, 2413 (1994).

[30] S. Nummela, P. Baumann, E. Caurier, P. Dessagne, A. Jokinen, A. Knipper, G. Le Scornet, C. Miehé, F. Nowacki, M. Oinonen, Z. Radivojevic, M. Ramdhane, G. Walter, J. Äystö, and the ISOLDE Collaboration, Phys. Rev. C **63**, 044316 (2001).

[31] GEANT – Detector description and simulation tool, version 3.21, CERN Program Library Long Writeup W5013, 1994.

[32] V. Maddalena, Ph. D. thesis, Michigan State University, 2000.

[33] D. R. Goosman, C. N. Davids, and D. E. Alburger, Phys. Rev. C **8**, 1324 (1973).

[34] L. K. Fifield, C. L. Woods, W. N. Catford, R. A. Bark, P. V. Drumm, and K. T. Keoghan, Nucl. Phys. A **453**, 497 (1986).

[35] A. Poves and J. Retamosa, Nucl. Phys. A **571**, 221 (1994).

[36] Y. Utsuno, T. Otsuka, T. Mizusaki, and M. Honma, Phys. Rev. C **60**, 054315 (1999).

[37] T. Nakamura, S. Shimoura, T. Kobayashi, T. Teranishi, K. Abe, N. Aoi, Y. Doki, M.

Fujimaki, N. Inabe, N. Iwasa, K. Katori, T. Kubo, H. Okuno, T. Suzuki, I. Tanihata, Y. Watanabe, A. Yoshida, and M. Ishihara, Phys. Lett. B **331**, 296 (1994).

[38] J. E. Bush, P. A. Hausladen, D. P. Balamuth, K. R. Pohl, D. Bazin, J. A. Brown, J. A. Caggiano, L. L. Chen, B. S. Davids, D. J. Morrissey, B. M. Sherrill, and M. Thoennessen, Phys. Rev. Lett. **81**, 61 (1998)

[39] A. Bonaccorso, I. Lhenry, and T. Suomijärvi, Phys. Rev. C **49**, 329 (1994).

[40] A. Bonaccorso and G. F. Bertsch, Phys. Rev. C **63**, 044604 (2001).

[41] W. F. Mueller, J. A. Church, T. Glasmacher, D. Gutknecht, G. Hackman, P. G. Hansen, Z. Hu, K. L. Miller, and P. Quirin, Nucl. Instrum. Methods A **466**, 492 (2001).

TABLES

TABLE I. Characteristics of the secondary beams and data acquisition time.

	^{34}Si	^{35}Si	^{37}S
Average secondary beam energy (A MeV)	73.4	73.8	69.2
Secondary beam intensity (s^{-1})	2 200	260	10^5
Beam purity (%)	66	92	87
Data acquisition time (h)	6.0	33.8	6.2

TABLE II. Single-neutron removal cross sections for the ^{9}Be(^{34}Si,^{33}Si)X reaction at 73 A MeV. Given are the experimental and theoretical excitation energies in the residual nucleus, $E_{\mathrm{x,Exp}}$ and $E_{\mathrm{x,Th}}$, the total angular momentum and parity of the final state J^{π}, the major quantum number, orbital and total angular momentum $N\ell j$ of the removed particle (as predicted from the shell model), predicted stripping ($\sigma_{\mathrm{sp}}^{\mathrm{str}}$) and diffraction cross sections ($\sigma_{\mathrm{sp}}^{\mathrm{diff}}$) for neutron knockout as calculated within the eikonal model (Eik) and the transfer to the continuum model (TC), the spectroscopic factor C^2S as calculated within the shell model, the total theoretical cross section σ_{Th} and the measured cross section σ_{Exp}. The J^{π} values in parentheses are suggested by theory. States above the neutron separation energy in ^{33}Si (S_{n} = 4.48 MeV) cannot be detected in the experiment and have not been included in the sum (lowest row).

$E_{\mathrm{x,Exp}}$	$E_{\mathrm{x,Th}}$	J^{π}	$N\ell j$	$\sigma_{\mathrm{sp,Eik}}^{\mathrm{str}}$	$\sigma_{\mathrm{sp,Eik}}^{\mathrm{diff}}$	$\sigma_{\mathrm{sp,TC}}^{\mathrm{str}}$	$\sigma_{\mathrm{sp,TC}}^{\mathrm{diff}}$	C^2S_{Th}	$\sigma_{\mathrm{Th,Eik}}$	$\sigma_{\mathrm{Th,TC}}$	σ_{Exp}
(MeV)	(MeV)	($\hbar$)	($\hbar$)	(mb)	(mb)	(mb)	(mb)		(mb)	(mb)	(mb)
0.00	0.00	$3/2^{+}$	$0d_{3/2}$	11.4	3.6	9.6	2.5	3.56	53	43	67(10)
1.01	0.85	$1/2^{+}$	$1s_{1/2}$	15.2	5.6	15.8	4.8	1.46	30	30	41(5)
		$(7/2^{-})$	$0f_{7/2}$	10.9	3.2						
	3.99	$(7/2^{+})$									
4.29(14)	4.38	$(5/2^{+})$	$0d_{5/2}$	9.0	2.5	7.6	1.6	2.50	29	23	15(3)
	4.42	$(3/2^{+})$	$0d_{3/2}$	8.9	2.5			0.11	$\sim$1		
	4.69	$(3/2^{+})$	$0d_{3/2}$	8.8	2.5			<0.01	(0)		
	4.93	$(1/2^{+})$	$1s_{1/2}$	11.7	3.8			0.42	(6)		
Σ									≈ 113	≈ 96	123(14)

TABLE III. Spectroscopic factors for neutron removal from ^{34}Si to specific final states in ^{33}Si. Given are the excitation energy of the final state E_x, the quantum numbers of the removed particle ($N\ell j$), and the spectroscopic factor predicted in the shell model $C^2S_{\rm Th}$. The experimental spectroscopic factor denoted $C^2S_{\rm Exp}$ was obtained by dividing the measured cross section by the (eikonal) single-particle cross section.

E_x[a]	$N\ell j$	$C^2S_{\rm Th}$	$C^2S_{\rm Exp}$
0 MeV	$0d_{3/2}$	3.56	4.5(7)
1.010 MeV	$1s_{1/2}$	1.46	2.0(3)
4.32(3) MeV	$0d_{5/2}$	2.50	1.3(4)

[a]Adopted values.

TABLE IV. Neutron-target optical potential parameters used in the transfer to the continuum calculations. For the parameterization of the potential see, e. g., Ref. [39].

	Strength (MeV)	Range (fm)	Diffuseness (fm)
Real	28	1.2	0.387
Imaginary	27.9 (surface) / 6.9 (volume)	1.368	0.3
Spin-Orbit	5.5	1.15	0.5

TABLE V. Electromagnetic transitions in ^{34}Si following the neutron knockout from ^{35}Si. The energies of the γ-ray transitions have been taken from [30]. Shown are the photon energy E_γ, possible initial and final states (angular momentum, parity, and excitation energy), and the probability for emitting a specific γ ray in the knockout process from a fit to the experimental spectrum (see Fig. 5). Question marks indicate ambiguities in the level scheme.

E_γ (keV)	$J_i^\pi; E_{x,i}$ ($\hbar$;keV)	$J_f^\pi; E_{x,f}$ ($\hbar$;keV)	b (%)
123	$(3^-,4^-,5^-);4379$	$3_1^-;4257$	—
591	$(3^-,4^-,5^-);4970$	$(3^-,4^-,5^-);4379$	14(3)
929	$3_1^-;4257$	$2_1^+;3326$	33(4)
1053	$(3^-,4^-,5^-);4379$?	$2_1^+;3326$?	4(2)
1193	$2_1^+;3326$?	$(0_2^+);2133$?	8(2)
1715	?	?	12(4)
2696	?	?	5(2)
3326	$2_1^+;3326$	$0_1^+;0$	54(3)
4257	$3_1^-;4257$	$0_1^+;0$	7(1)

TABLE VI. Same as Table II for the ^{9}Be(^{35}Si,^{34}Si)X reaction. Experimental cross sections are not given since the level scheme is experimentally unclear. Values of J^{π} in parentheses are suggested from theory. All states predicted from a spherical shell-model calculation below the particle emission threshold in ^{34}Si at $S_{\rm n} = 7.54$ MeV with a spectroscopic factor $C^2S > 0.02$ are listed. The eikonal model has been used to calculate the single-particle cross sections.

$E_{\rm x,Exp}$ (MeV)	$E_{\rm x,Th}$ (MeV)	J^{π} ($\hbar$)	$N\ell j$ ($\hbar$)	$\sigma^{\rm str}_{\rm sp,Eik}$ (mb)	$\sigma^{\rm diff}_{\rm sp,Eik}$ (mb)	$C^2S_{\rm Th}$	$\sigma_{\rm Th}$ (mb)
0.00	0.00	0^+	$0f_{7/2}$	15.6	5.6	0.86	18
3.33	—	2^+	—	—	—	—	—
4.26	3.98	3^-	$0d_{3/2}$	11.5	3.7	0.63	10
			$1s_{1/2}$	16.9	6.6	0.11	3
—	3.82	(4^-)	$0d_{3/2}$	11.4	3.7	0.94	14
—	4.28	(5^-)	$0d_{3/2}$	11.0	3.5	1.19	17
—	4.70	(3^-)	$1s_{1/2}$	16.0	6.1	0.55	12
—	4.89	(2^+)	$0f_{7/2}$	11.2	3.3	0.07	1
—	4.90	(2^-)	$0d_{3/2}$	10.9	3.4	0.47	7
—	5.53	(4^-)	$1s_{1/2}$	15.1	5.5	0.77	16
—	7.10	(2^-)	$0d_{5/2}$	9.3	2.5	0.04	0
Σ							98

FIGURES

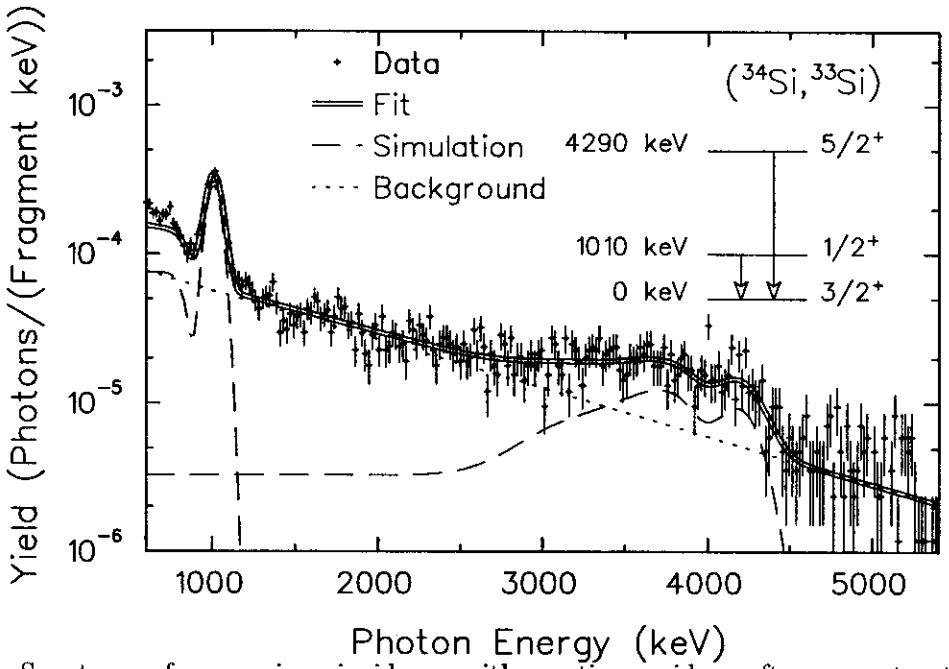

FIG. 1. Spectrum of γ rays in coincidence with reaction residues after reconstruction of the center-of-mass energy. The data (points) are well described by a continuous background parameterized as a single exponential (dotted) and by line shapes deduced from Monte-Carlo simulations (dashed). Two transitions could be identified. The overall fit is shown as a double solid line. The inset shows a simplified level scheme.

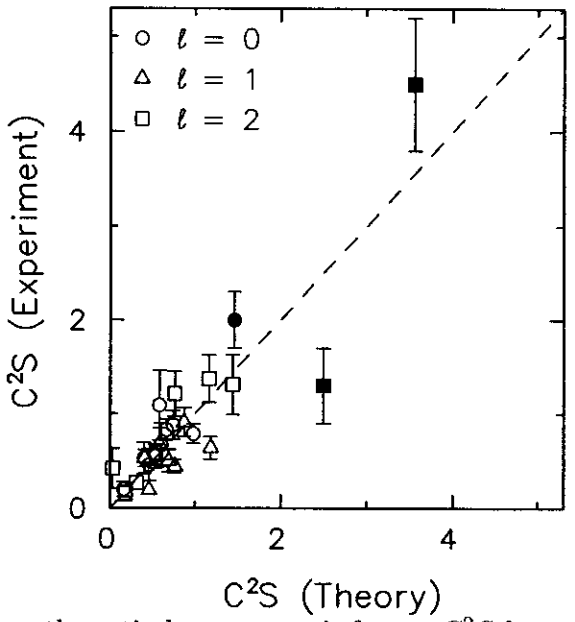

FIG. 2. Experimental vs. theoretical spectroscopic factors C^2S from all cases studied so far, see [12], and including results from the present work (full symbols). The experimental values represent the measured partial cross section divided by the single-particle cross section (from the eikonal calculation). The theoretical values are from many-body shell-model calculations. The dashed line is the diagonal indicating that these two, basically unrelated, quantities are connected by a scale factor of order unity.

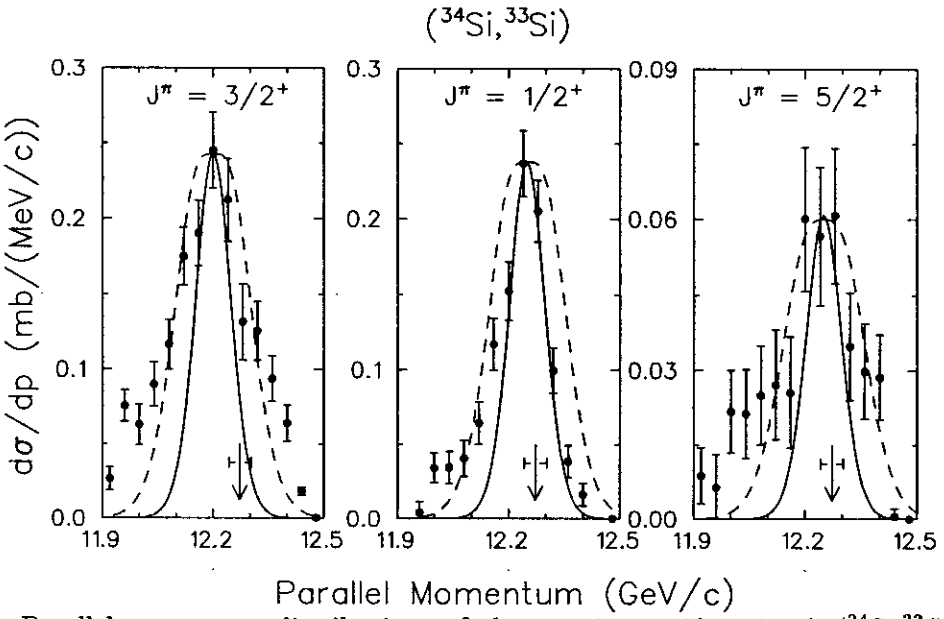

FIG. 3. Parallel-momentum distributions of the reaction residues in the(^{34}Si,^{33}Si) reaction leading to final states at 0 (left), 1.01 (middle), and 4.32(3) MeV (right). The data (full points) are compared with theoretical estimates from an eikonal approximation [15] for $\ell = 0$ removal (solid) and $\ell = 2$ removal (dashed). The heights and centroids of the theoretical curves have been scaled to match the data. From the shapes the angular-momentum values are seen to be $\ell = 2$, 0, 2 in agreement with the assignments $J^\pi = 3/2^+, 1/2^+, 5/2^+$. The calculations take the mid-points of the distributions to be 12.20, 12.25 and 12.25 GeV/c, respectively. If the fragments were produced with a distribution centered at the velocity of the projectile the expected mid-point would be 12.27(3) GeV/c, indicated by the arrows.

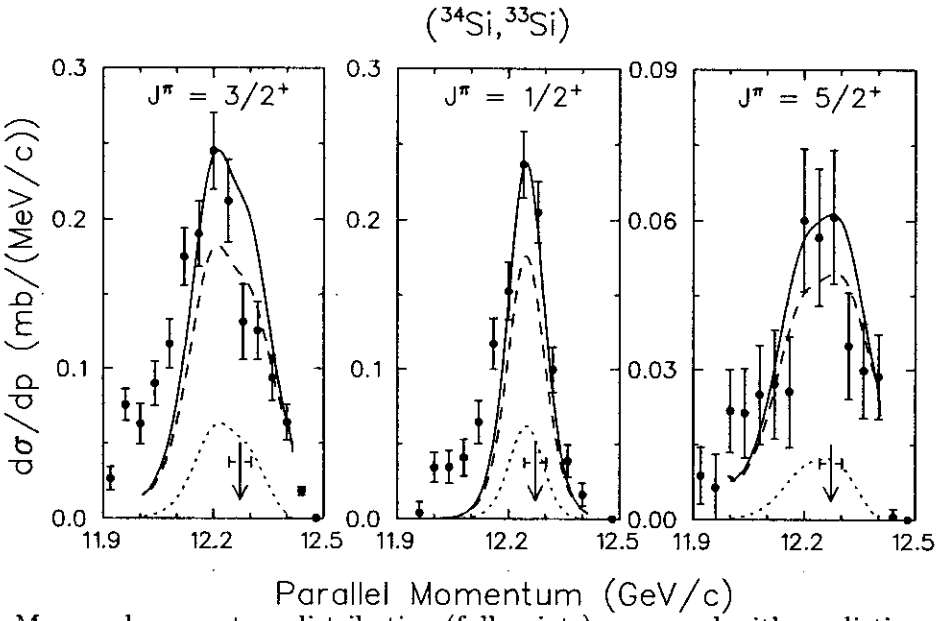

FIG. 4. Measured momentum distribution (full points) compared with predictions within the transfer-to-the-continuum model according to [20] for the (^{34}Si,^{33}Si) reaction leading the the ground state (left), the 1.01 MeV state (middle), and the 4.32 MeV state (right). The full curves show the total neutron removal cross section in comparison to stripping (dashed) and diffraction breakup (dotted), all calculated for the same incident beam energy of 70.6 A MeV corresponding to a momentum of 12.192 GeV/c in this figure. For the proposed $d_{3/2}$ removal the theoretical distribution has been scaled to match the data by a factor of 1.32, for $d_{5/2}$ by 0.7. The arrows indicate the momentum corresponding to experimental projectile velocity.

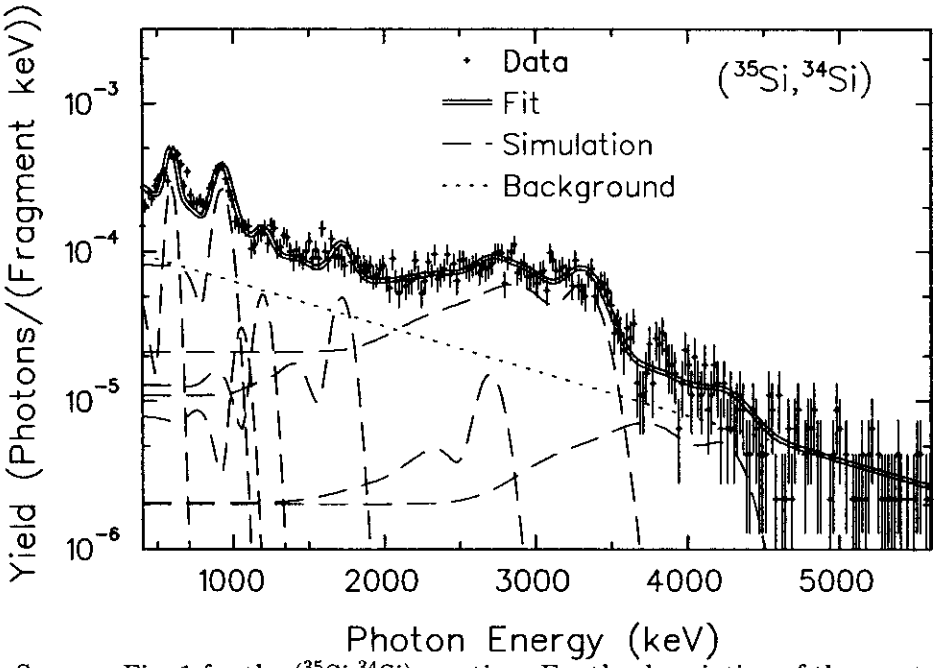

FIG. 5. Same as Fig. 1 for the (^{35}Si,^{34}Si) reaction. For the description of the spectrum, known transitions [30] in ^{34}Si have been used. The shape and absolute amount of background γ rays agrees with the result obtained from the (^{34}Si,^{33}Si) γ-ray spectrum.

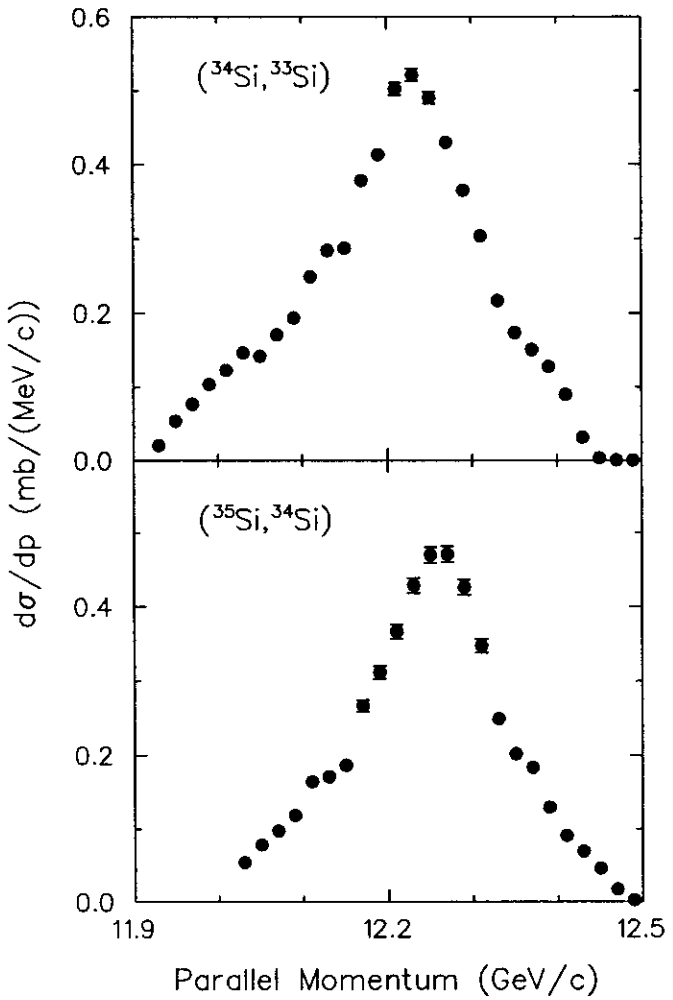

FIG. 6. Inclusive momentum distributions for the neutron knockout from ^{34}Si (upper part) and ^{35}Si (lower part).